

Wavelength injection locking actively Q-switched random fiber laser based on random phase-shifted fiber Bragg grating and electro-optic modulator*

PAN Honggang, ZHANG Bo, SONG Dianyou**, CHEN Zhipan, CHEN Chunqi, and LI Rupeng

School of Integrated Circuit Science and Engineering, Tianjin University of Technology, Tianjin 300384, China

(Received 11 July 2023; Revised 21 September 2023)

©Tianjin University of Technology 2024

In this paper, an actively Q-switched wavelength injection locking random fiber laser (RFL) based on random phase-shifted fiber Bragg grating (RPS-FBG) is proposed, and the performance of the laser is verified by experiments. Within the reflection bandwidth range of RPS-FBG, spanning from 1 549.2 nm to 1 549.9 nm, different laser modes with stable central wavelength and peak power can be selectively chosen by varying the injected light wavelength. The power fluctuation within 1 h is less than 0.1 dBm, and the central wavelength drift is less than 0.02 nm. When the pump power increases from 90 mW to 300 mW, the pulse width decreases from 3.2 μ s to 1.5 μ s, and the pulse repetition frequency is 20 kHz. The RFL can reach a stable locking state at the lowest pump power of 100 mW and the lowest injection power of 3 dBm. When the wavelength is locked, the output pulse is a single pulse. On the contrary, the unlocked output pulse is multi-pulse. The laser has the characteristics of high wavelength tunability in the reflection range of RPS-FBG and it can be an ideal light source in the fields of laser imaging and pulse coding.

Document code: A **Article ID:** 1673-1905(2024)03-0135-7

DOI <https://doi.org/10.1007/s11801-024-3127-0>

Since being proposed in 2010, random distributed feedback fiber lasers (RDF-FLs) have received extensive attention due to their high efficiency and simple structure^[1,2]. Compared with traditional fiber lasers based on cavity mirror feedback, random fiber laser (RFL) is based on the localized effect of light scattering in the fiber^[3]. It is characterized by a simple structure, superior directivity and stable output. Additionally, it can produce narrow linewidth laser output due to its distributed amplification effect. As a result, RFL finds diverse application prospects in the realms of imaging^[4], optical fiber sensing^[5] and nonlinear optics^[6].

Researchers frequently employ the nonlinear gain (stimulated Raman/Brillouin scattering amplification effect) of long single-mode fiber (SMF)^[7-9] as the foundation for the design of RDF-FLs. Furthermore, exploiting the capability of stimulated Brillouin scattering within SMF for wavelength conversion enables the attainment of stable multi-wavelength output in RFL systems through the substantial amplification of Brillouin pump power to excite higher order Brillouin Stokes light^[10,11]. Random lasers, however, often require tens of kilometers of SMF in order to provide effective feedback, and they have a high threshold for generating.

To shorten the length of the feedback medium and decrease the laser threshold, SHAPIRA et al^[12] used ran-

dom phase shift fiber Bragg grating (RPS-FBG) arrays to verify the optical localization phenomenon in their research, and explored its various applications in random lasers. After LIZARRAGA et al^[13] realizing a 150 cm erbium-germanium co-doped RFL with 31 FBGs pumped by 976 nm laser in 2009, GAGNÉ et al^[14] used some single FBGs with a length of 20—30 cm instead of random grating array to realize compact RFL, obtaining a laser output with a linewidth of 0.5 pm. Due to the effective optical localization effect introduced by FBGs and the high gain of erbium-doped fiber, the gain threshold of RFL reaches 3—10 mW.

Because the reflection wavelength phase of the RPS-FBG is random in the RDF-FL described above, controlling the output wavelength is difficult. To achieve switchable and tunable effects, in random lasers using SMF as the feedback medium, researchers usually use filters, such as Sagnac loop filters^[15], programmable optical processors (WaveShaper)^[16] and Bragg grating array^[17]. Thus, different filters can be used in RFL to obtain stable wavelengths. In 2019, ZHANG et al^[18] used the bean scanning method to apply a 20-mm-long RPS-FBG with 20 random phase shifts, by immersing the RPS-FBG into water to suppress the mode competition to obtain a more stable single-wavelength laser. However, this operation is too restrictive and cumbersome for

* This work has been supported by the National Natural Science Foundation of China (No.17JCYBJC16600/201386).

** E-mail: youdiansong@163.com

practical applications, and the mode competition can be suppressed to generate a stable single wavelength. However, the wavelengths cannot be adjusted individually.

Moreover, random pulse lasers are also a hot research area in recent years, which can be used in pulse coding and other fields. Pulse output can be achieved by passive methods such as saturable absorbers^[19], or by active methods. Active control mechanisms allow real-time control of the obtained pulse, and their repetition rates are very stable. Therefore, we introduce an electro-optic modulator (EOM) to realize active Q-switching. By adjusting the pump power and introducing injected light, single-pulse or multi-pulse output can be adjusted.

In this paper, RPS-FBG is used as the feedback medium to realize RFL. Through the EOM, active Q-switching is introduced into the injection locking system. The experimental results indicate whether the wavelength is locking is related to the pump optical power and the injected optical power. When the pump power is increased from 150 mW to 300 mW, the injected optical power is required to increase from 10 dBm to 14 dBm to achieve an injection-locked state. In addition, both pulse amplitude and spectral amplitude are affected by the central wavelength of the injected light. They reach the highest point when the injected light wavelength is 1 549.8 nm. When the injected optical power increases from 6 dBm to 12 dBm, the output pulse power is relatively stable, and the power is about 9 dBm.

Based on RPS-FBGs, the experimental setup of the actively Q-switched wavelength injection locking RFL is illustrated in Fig.1. A tunable wavelength laser TLS200 (with a wavelength tuning range of 1 528—1 565 nm and an output power adjustment range of 6—15 dBm) acts as seed light to inject into the cavity through a 3 dB optical coupler 2 (OC2) to lock the emission wavelength of the system laser. The RPS-FBG is connected to the cavity through circulator port 2 to provide feedback. Meanwhile, the unidirectional propagation of light in the cavity is ensured. It is a fiber-coupled LiNbO₃ EOM based on Mach-Zehnder (M-Z) structure with a 10 GHz modulation bandwidth and a maximum direct current (DC) bias voltage of 5 V. A 980 nm pump light source is used to pump a section of erbium-doped fiber (EDF) with a length of 10 m, core diameter and cladding diameter of 6/125 μm, and erbium ion doping concentration of 4 000 ppm through a 980 nm/1 550 nm wavelength division multiplexing (WDM). A polarization controller (PC) is used to control the polarization state of the light in the RFL, the 20% port of optical coupler 1 (OC1) is used for the output of the laser, and the 80% port is used for the feedback of the optical resonator. The output spectrum is analyzed using an optical spectrum analyzer (YOKOGAWA AQ6370D OSA) with a spectral resolution of 0.02 nm. The output power was measured by an optical power meter (PMSII-A). The time-domain characteristics of the laser are recorded through a 200 MHz digital oscilloscope (UTD4202C) in conjunction with a photo-

detector (Discovery Semiconductors, DSC10H, 200 MHz).

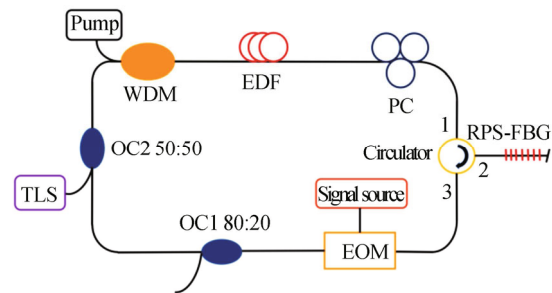


Fig.1 Experimental setup of wavelength injection locking active Q-switched RFL based on RPS-FBG

The transmission spectrum and reflection spectrum of the RPS-FBG used in the experimental setup are shown in Fig.2. The RPS-FBG is fabricated by the beam scanning method, by introducing 20 phase-shift points with random changes into an ultra-short grating with a length of 25 mm, the central wavelength is about 1 550 nm, and each grating is about 1.19 mm. Due to the similar characteristics of the grating segments, it has a similar reflectivity, and the reflectivity is about 4%. It can be seen from Fig.2 that the bandwidth of the reflection spectrum is slightly wider than that of the transmission spectrum, and the 3 dB bandwidth centered at 1 549.55 nm is 0.70 nm. As a result of the randomness of the feedback provided by the random grating, many narrow linewidth transmission spikes appear on the reflection spectral envelope, which can introduce intense mode competition in random lasers, affecting the stability of the laser output.

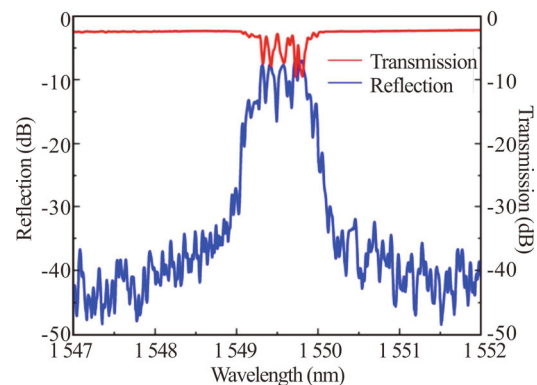


Fig.2 Reflection and transmission spectra of the RPS-FBG

When the pump power is 300 mW, the external modulation signal is a sine wave with a frequency of 20 kHz and a modulation amplitude of 5 V, the output spectra are sampled every 10 min, and a total of six spectra are collected in different moments. When the pump power is fixed at 300 mW, the output spectrum is dual-wavelength by adjusting the polarization angle of PC, and the output spectrum hardly changes. As shown in Fig.3(a), two dynamic output peaks are visible in the spectra of RFL.

With RPS-FBG as the feedback medium, the RFL has no constant laser resonator and no fixed output modes, and multiple laser modes coexist. It can be seen from the reflection spectrum in Fig.2 that there are many random resonance peaks. As a result, there is intense mode competition in the cavity, causing the output of the RFL to fluctuate significantly. When a narrow linewidth laser with a center wavelength of 1 549.5 nm and a power of 6 dBm is injected into the RFL under fixed pump power, the injection locking phenomenon is observed. And as shown in Fig.3(b), the spectra are also sampled every 10 min, and a stable single-wavelength laser with the central wavelength shift of less than 0.02 nm is obtained within a 1 h observation period. This is because adding the injected light replaces the original fierce mode competition with a stronger mode resonance.

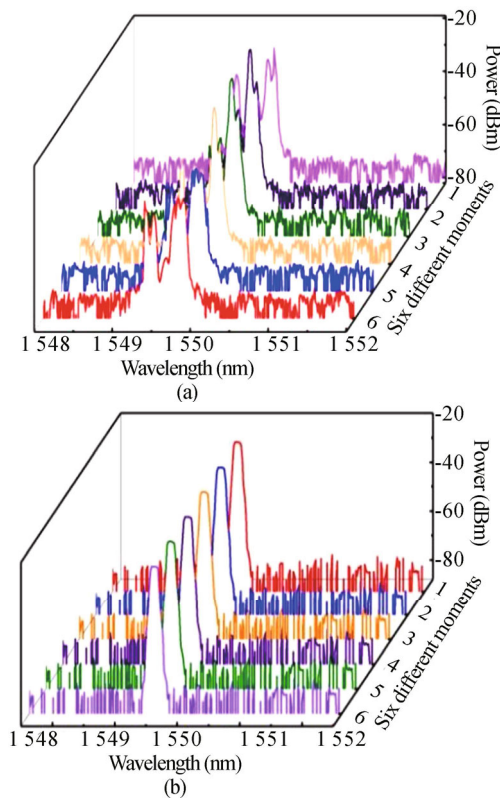


Fig.3 Output spectra at six different moments when pump power is 300 mW: (a) Without injected light; (b) With injected light

Fig.4 illustrates the output spectrum of the RFL under the influence of different injected wavelengths when the pump power is set to 300 mW and the injected optical power is at 6 dBm. By adjusting the TLS, we can obtain a narrow linewidth laser whose central wavelength can be adjusted from 1 549.2 nm to 1 549.9 nm. It shows that the output wavelength of the laser can be controlled by the wavelength of the injected light. Its range is consistent with that of the RPS-FBG reflection spectrum, which also confirms that within the reflection spectrum range of RPS-FBG, the injected light can lock the output

of the RFL, and it exhibits good wavelength stability.

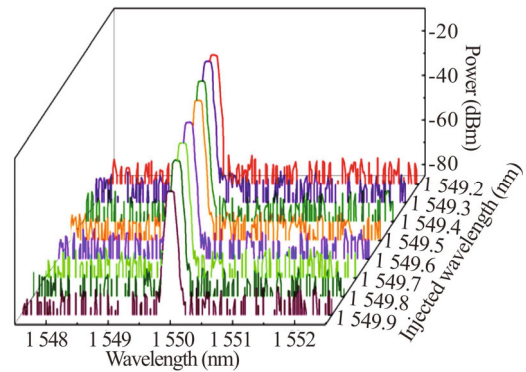


Fig.4 Output spectra corresponding to different injection wavelengths when pump power is 300 mW and injection power is 6 dBm

In order to further explore the effects of the pump power and the injection power on injection locking, we adjust the TLS to output a laser with a central wavelength of 1 549.5 nm. Fig.5(a) shows the output spectrum of RFL when the TLS injection power is 6 dBm and the pump power is changed from 90 mW to 300 mW. It can be observed that when the pump power is 90 mW, the output spectrum is a single wavelength output with a central wavelength of 1 549.5 nm. The injected light, however, can not eliminate the fierce mode competition in the cavity completely with the increase of the pump power. A pump power of 200 mW produces an output wavelength with many unstable peaks at 1 549.8 nm. As the pump power continues to rise, when it was 300 mW, dual-wavelength output with peaks appearing at 1 549.5 nm and 1 549.8 nm, and the injection locking has basically failed at this point. Fig.5(b) exhibits the spectra of the TLS under varying injection powers while maintaining a pump power of 200 mW. It is observed that the occurrence of dual wavelengths resulting from mode competition becomes progressively subdued as the injection power is elevated.

From above experiments, we can conclude it is clear that the wavelength locking is dependent on both the pump power and the injected optical power. Through further experiments, the wavelength-locked injected optical power thresholds under different pump powers can be obtained, as shown in Fig.6. With the gradual increase of the pump power, achieving locking necessitates a higher injected optical power. The phenomenon of injection locking manifests at the critical value along the curve. For instance, in the case of a pump power of 150 mW, a stable injection locking can be achieved by applying an injection optical power of 10 dBm, and it will not happen if the injected optical power is less than 10 dBm. When the pump power is 100 mW, only about 3 dBm of injected optical power is needed to generate locking. The injected optical power threshold for wavelength locking is positively correlated with the pump optical power. In other words, the injected optical power

must increase along with the pump optical power to lock the resonance wavelength for the stable output. The reason for this phenomenon is that higher pump power stimulates more laser modes in the cavity of the RFL, making wavelength locking more difficult. In this case, a higher injected optical power is required to enhance the resonant intensity of a specific mode, and then through mode resonance suppression of other laser modes, achieving the effect of injection locking.

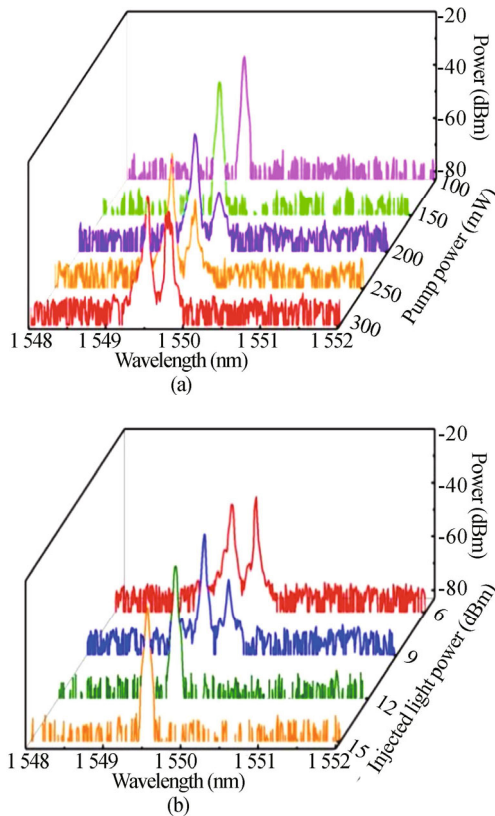


Fig.5 (a) Output spectra at pump power from 90 mW to 300 mW; (b) Output spectra at injected light power from 6 dBm to 15 dBm

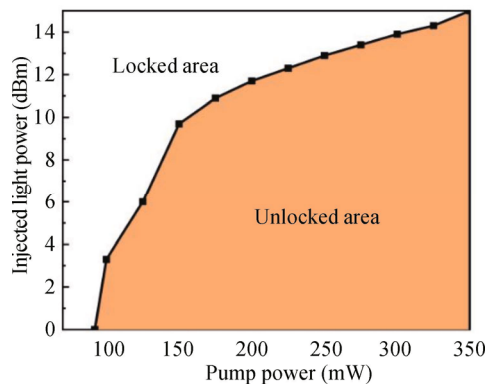


Fig.6 The curve depicting the relationship between pump power (from 92 mW to 300 mW) and injected light power (from 6 dBm to 15 dBm) threshold for wavelength locking

In this paper, active Q-switching is introduced into

RFL through a fiber-coupled LiNbO₃ EOM based on M-Z structure. The modulation signal is a sine wave with a frequency of 20 kHz and a modulation amplitude of 5 V. As shown in Fig.7, it can be found that in the RPS-FBG reflection spectrum range from 1 549.2 nm to 1 549.9 nm, different injection wavelengths correspond to different output spectral intensities and pulse amplitudes. It can be found that the highest spectral intensity and pulse amplitude both appear at the wavelength of 1 549.8 nm. The spectral amplitudes and pulse amplitudes at 1 549.2 nm and 1 549.9 nm at the edge of the reflection spectrum are significantly lower than the rest.

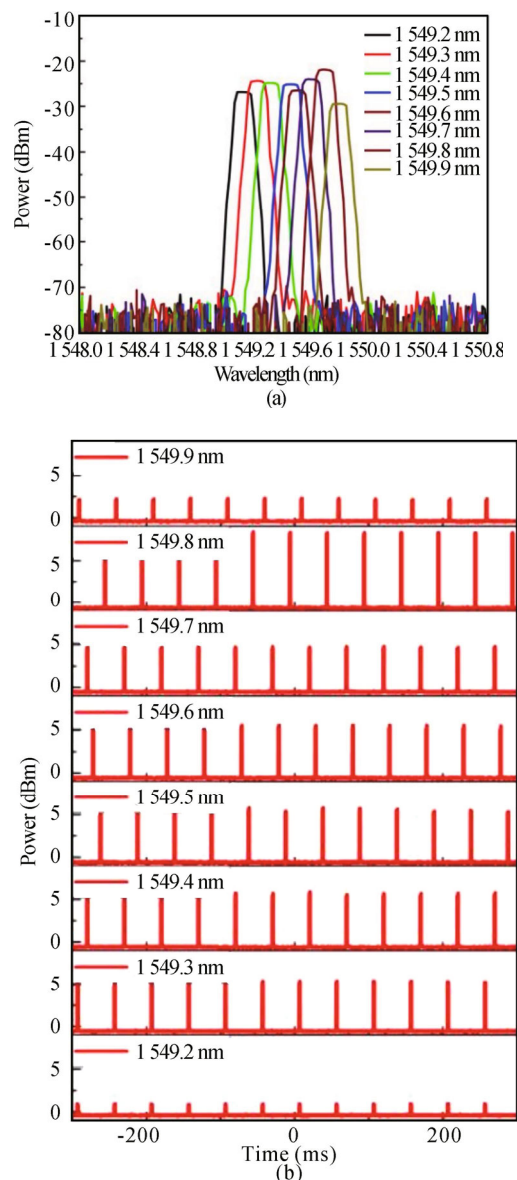


Fig.7 (a) Output spectra at different injection wavelengths with the pump power of 300 mW, the injection power of 6 dBm, the external modulation signal of a sine wave with a frequency of 20 kHz and a modulation amplitude of 5 V; (b) Output pulse sequences at different injection wavelengths

As shown in Fig.8, under pump power of 300 mW,

central wavelength of the injecting narrow linewidth laser is 1 549.8 nm. In Fig.9 and Fig.10, the external modulation signal is a sine wave with a frequency of 20 kHz and a modulation amplitude of 5 V, when the power of the injected signal is increased from 6 dBm to 12 dBm. During the whole experiment, the laser is in injection locking state. As shown in Fig.9, it can be found that the change of the output pulse amplitude is not obvious, and the pulse intervals are also unchanged. In addition, as can be seen from Fig.10, the pulse width of the output pulse remains at about 2.5 μ s. Consequently, injection power has little effect on output pulses.

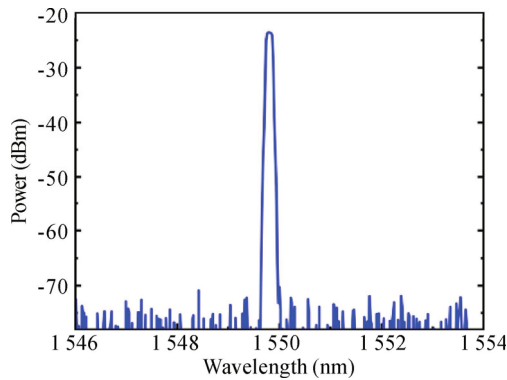


Fig.8 Output spectrum when fixed pump power at 300 mW, and central wavelength of the injecting narrow line-width laser is 1 549.8 nm

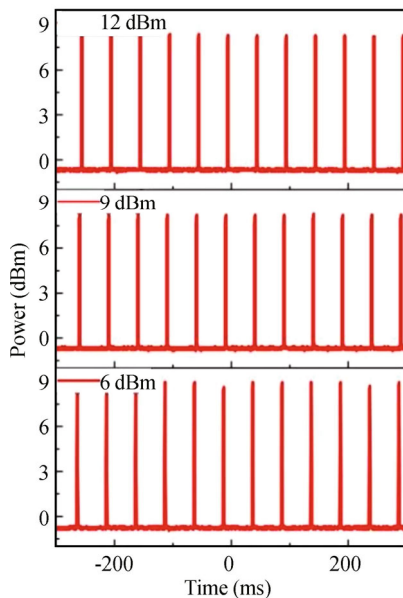


Fig.9 Output pulses at different injection powers when the pump power is 300 mW, the injection wavelength is 1 549.8 nm, and the external modulation signal is a sine wave with a frequency of 20 kHz and a modulation amplitude of 5 V

Fig.11 shows the variation trend of output power and pulse width under different pump powers. The red curve is the relationship between pump power and output power, and the black curve is the relationship between

pump power and pulse width. The pump power and output power are approximate linearity relation. With increasing pump power, the pulse width gradually decreases. At the same time, the pulse width is affected by the rise time of EOM and the dynamic gain of the EDF. When the laser is transmitted back and forth in the RFL, the generated pulse peak will continuously and rapidly exhaust the superior particles, resulting in a pulse with narrow pulse width. As the pump power increases, the Q value in the cavity is increasingly higher, so is the depletion rate faster, resulting in the narrowing of pulse width^[20]. Combined with the description of Fig.8 and Fig.9, we can conclude that the pulse width in RFL is only affected by the pump power, and has nothing to do with the injection power.

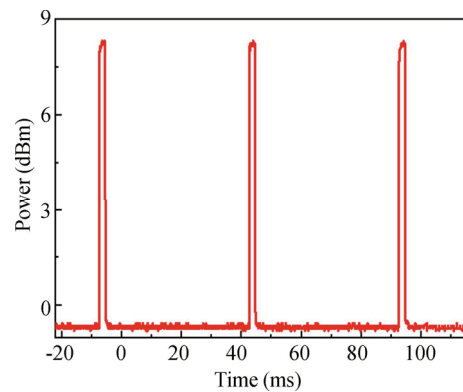


Fig.10 Output pulses at injection power of 12 dBm when the pump power is 300 mW, the injection wavelength is 1 549.8 nm, and the external modulation signal is a sine wave with a frequency of 20 kHz and a modulation amplitude of 5 V

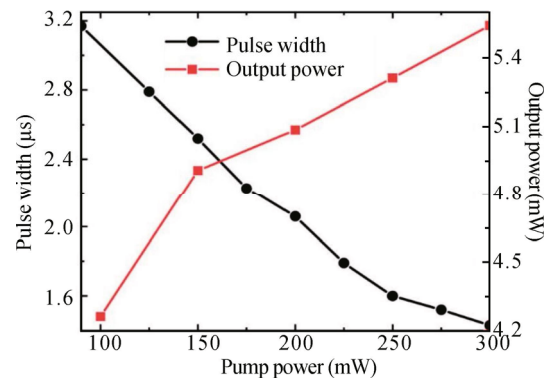


Fig.11 Variations of output power and pulse width when the pump power is changed from 92 mW to 300 mW

Furthermore, in the absence of wavelength locking of the RFL, the generation of a random pulse sequence ensues. A RFL pulse sequence was shown in Fig.12(a) with a pump power of 300 mW, an injected optical power of 12 dBm, a wavelength of 1 549.8 nm, and a modulation signal as a sine wave with a frequency of 20 kHz and an amplitude of 5 V. Due to wavelength locking, there is only one resonance wavelength as shown in Fig.12(b), and the output pulse sequence is a stable single pulse

signal produced by EOM modulation.

When the pump power is set at 300 mW, the injected optical power amounts to 6 dBm, while the injected wavelength corresponds to 1 549.8 nm. The wavelength injection locking phenomenon does not occur, thus random pulse trains can be observed. As shown in Fig.12(c), due to the lack of wavelength locking as well as the beat frequencies between 1 549.5 nm, 1 549.8 nm and the injected light, there is fierce mode competition within the RFL. At the same time, due to the high pump power and high repetition frequency, the output pulses are split and there are multiple output pulses in one cycle. Moreover, because the output light is generated by the RPS-FBG as a feedback medium, it is highly random and unstable, resulting in amplitude imbalance in multi-pulse sequences. Because there is no wavelength locking, the output spectrum is dual-wavelength, as shown in Fig.12(d).

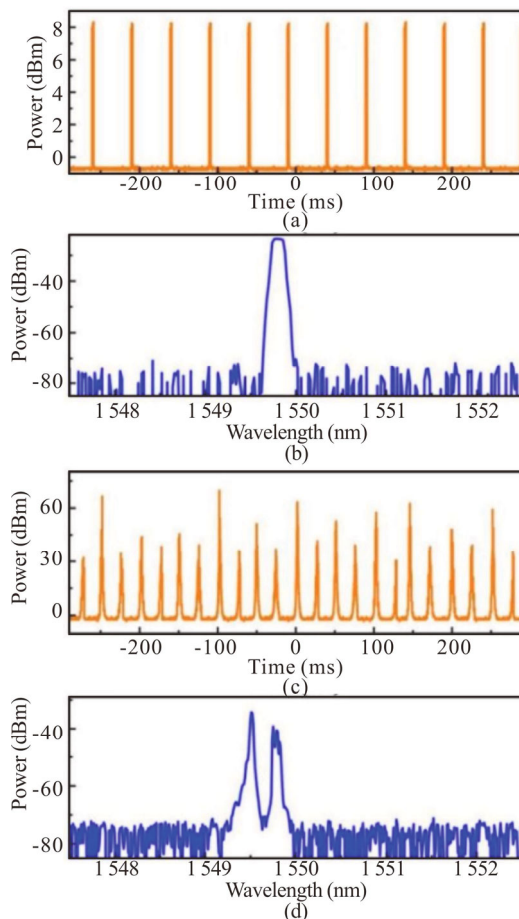


Fig.12 Output pulses in different states of (a) locking and (c) not locking; Output spectra in different states of (b) locking and (d) not locking

This paper presents a novel approach to achieve wavelength injection locking in a RFL utilizing a tunable random phase shift grating. The RPS-FBG employed in this configuration exhibits a reflection range spanning from 1 549.2 nm to 1 549.9 nm. A semi-open cavity RFL is constructed using a RPS-FBG as the feedback me-

dium. When no seed light is injected, the instability of the output wavelength arises from the presence of mode competition. However, by introducing seed light injection, a stable and singular output wavelength can be achieved. By observing the output spectrum and the output pulse, both of them obtained the highest value at 1 549.8 nm. When wavelength locking, the pulse width decreases with increasing pump power. The wavelength injection locking RFL based on RPS-FBG proposed in this paper has the characteristics of simple structure, stable single wavelength after locking and easy control over the central wavelength. The stable and easily controllable single wavelength can be used in fields such as medical and laser imaging. And due to the introduction of the EOM, there is a stable single pulse after injection locking, which can be used in pulse coding, pulse sequence laser detection and other technical fields.

Ethics declarations

Conflicts of interest

The authors declare no conflict of interest.

References

- [1] SERGEI K, SERGEY A, DMITRY V, et al. Random distributed feedback fibre lasers[J]. *Physics reports*, 2014, 542(2): 133-193.
- [2] ZHU J M, ZHANG W L, RAO Y J, et al. Output characteristics of low-threshold random distributed feedback fiber laser[J]. *Chinese journal lasers*, 2013, 40(3): 302007. (in Chinese)
- [3] ZHENG W Z, HONG L L, CHEN W, et al. Low threshold short cavity random distributed feedback fiber laser[J]. *Laser & infrared*, 2016, 46(1): 48-51.
- [4] MA R, RAO Y J, ZHANG W L. Multimode random fiber laser for speckle-free imaging[J]. *IEEE journal of selected topics in quantum electronics*, 2019, 25(1): 0900106.
- [5] DENG J C, CHURKIN D V, XU Z W. Random fiber laser based on a partial-reflection random fiber grating for high temperature sensing[J]. *Optics letters*, 2021, 46(5): 957-960.
- [6] WANG F, YU W, TIAN J. 5.1 kW tandem-pumped fiber amplifier seeded by random fiber laser with high suppression of stimulated Raman scattering[J]. *IEEE journal of selected topics in quantum electronics*, 2021, 27(21): 6800109.
- [7] XU Y, GAO S, LU P, et al. Low-noise Brillouin random fiber laser with a random grating-based resonator[J]. *Optics letters*, 2016, 41(14): 3197-3200.
- [8] ZHANG L, XU Y, LU P, et al. Multi-wavelength Brillouin random fiber laser via distributed feedback from a random fiber grating[J]. *Journal of lightwave technology*, 2018, 36(11): 2122-2128.
- [9] HUANG P, DU Y, SHU X, et al. Half-open-cavity multi wavelength Brillouin-erbium random fiber laser with improved performance[J]. *Laser physics*, 2020, 30(3): 035101.

- [10] ZHOU Y, GAO P, ZHANG X, et al. Switchable multi wavelength erbium-doped fiber laser based on a four-mode FBG[J]. Chinese optics letters, 2019, 17(1): 010604.
- [11] WANG F, GONG Y. Tunable and switchable multi wavelength erbium-Brillouin random fiber laser incorporating a highly nonlinear fiber[J]. Journal of light-wave technology, 2020, 38(15): 4093-4099.
- [12] SHAPIRA O, FISCHER B. Localization of light in a random grating array in a single mode fiber[J]. Journal of the optical society of America B, 2005, 22(12): 2542-2552.
- [13] LIZÁRRAGA N, PUENTE N P, CHAIKINA E I. Single-mode Er-doped fiber random laser with distributed Bragg grating feedback[J]. Optics express, 2009, 17(2): 395-404.
- [14] GAGNÉ M, KASHYAP R. Demonstration of a 3mW threshold Er-doped random fiber laser based on a unique fiber Bragg grating[J]. Optics express, 2009, 17(21): 19067-19074.
- [15] PAN H G, GUO T T, ZHANG A L, et al. Multi-wavelength switchable random fiber laser based on double Sagnac-loop filter[J]. Journal of modern optics, 2021, 68(17): 945-952.
- [16] SUN C, PAN H G, ZHANG A L, et al. Effects of dispersion on characterization of multi-wavelength Q-switched fiber laser[J]. Optics communications, 2020, 462(1): 125373.
- [17] ZHU Y Y, ZHANG W L, JIANG Y. Tunable multi-wavelength fiber laser based on random Rayleigh back-scattering[J]. IEEE photonics technology letters, 2013, 25(16): 1559-1561.
- [18] ZHANG A L, HAO L Y, GENG B. Investigation of narrow band random fiber ring laser based on random phase-shift Bragg grating[J]. Optics & laser technology, 2019, 116(1): 1-6.
- [19] MENG Y, ZHANG S, LI X. Graphene Q-switched fiber laser with broadband, random, multimode oscillation[J]. Optik, 2015, 126(24): 5253-5255.
- [20] YU Y, WEI X M, KANG J Q, et al. Pulse-spacing manipulation in a passively mode-locked multipulse fiber laser[J]. Optics express, 2017, 25(12): 13215-13221.